This document is downloaded from DR-NTU (https://dr.ntu.edu.sg)
Nanyang Technological University, Singapore.

Improved adsorption characteristics data for AQSOA types zeolites and water systems under static and dynamic conditions

Teo, How Wei Benjamin; Chakraborty, Anutosh; Fan, Wu

2017

Teo, H. W. B., Chakraborty, A., & Fan, W. (2017). Improved adsorption characteristics data for AQSOA types zeolites and water systems under static and dynamic conditions. Microporous and Mesoporous Materials, 242, 109-117.

https://hdl.handle.net/10356/82304

https://doi.org/10.1016/j.micromeso.2017.01.015

© 2017 Elsevier. This is the author created version of a work that has been peer reviewed and accepted for publication by Microporous and Mesoporous Materials, Elsevier. It incorporates referee’ s comments but changes resulting from the publishing process, such as copyediting, structural formatting, may not be reflected in this document. The published version is available at: [http://dx.doi.org/10.1016/j.micromeso.2017.01.015].

Downloaded on 19 Jul 2024 03:50:13 SGT

Improved Adsorption Characteristics Data for AQSOA Types Zeolites and Water Systems under Static and Dynamic Conditions

How Wei Benjamin Teo[1], Anutosh Chakraborty[1,*], Wu Fan[1]

[1]School of Mechanical and Aerospace Engineering, Nanyang Technological University, 50 Nanyang Avenue Singapore, 639798

[*]Author to whom correspondence should be addressed,

E-mail: AChakraborty@ntu.edu.sg, Tel: +65 6790 4222

Graphical Abstract

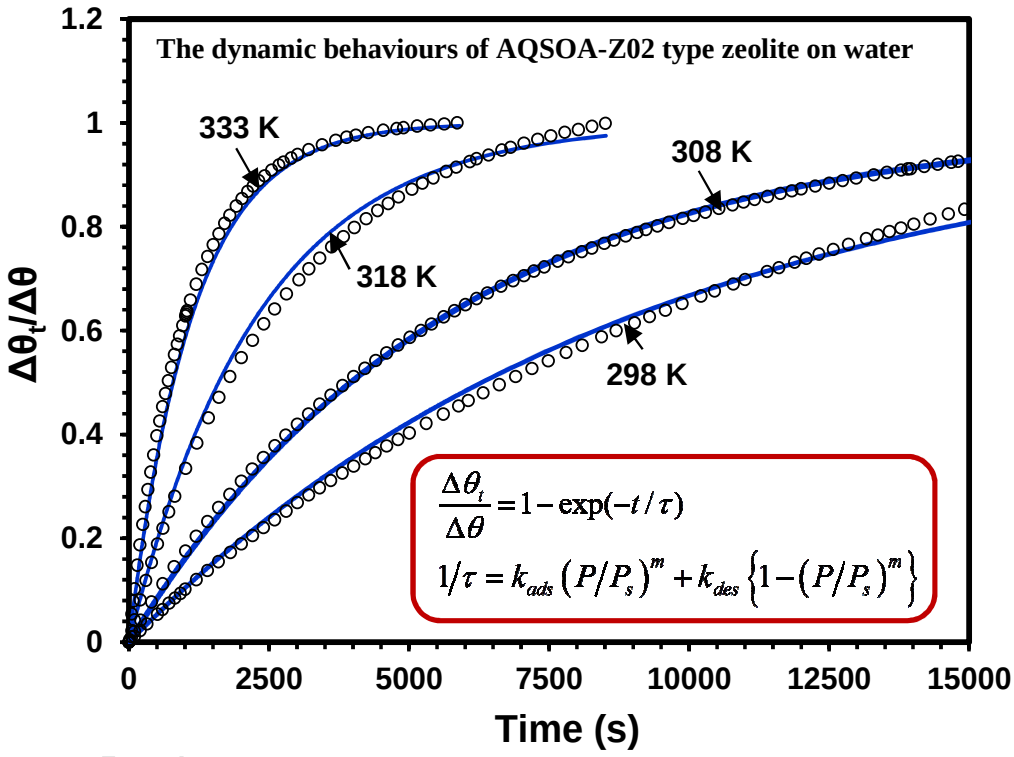

ACCEPTED MANUSCRIPT

Improved Adsorption Characteristics Data for AQSOA Types Zeolites and Water Systems under Static and Dynamic Conditions

How Wei Benjamin Teo[1], Anutosh Chakraborty[1,*], Wu Fan[1]

[1]School of Mechanical and Aerospace Engineering, Nanyang Technological University, 50 Nanyang Avenue Singapore, 639798

[*]Author to whom correspondence should be addressed,

E-mail: AChakraborty@ntu.edu.sg, Tel: +65 6790 4222

Abstract

In this manuscript, the amount of water vapour uptakes on zeolites (types AQSOA-Z01, Z02 and Z05) under static and dynamic conditions were measured for the temperatures ranging from 298K to 333K and pressures up to saturation conditions. These data are fitted with the theoretical isotherms and kinetics equations, which are developed from Langmurian analogy. The experimentally measured isotherms data varying from Henry's region to the saturated pressure are also expressed in pressure–temperature–uptake co-ordinate system for the calculation of the isosteric heat of adsorption. The variations of isosteric heats are ranged from 1 to 1.4 times of the heat of vaporization. The AQSOA type zeolites show type V isotherms. For better understanding of adsorption and desorption processes, the hysteresis behaviours are also investigated.

1. Introduction

The demands for air-conditioning cooling in summer are increased tremendously as the living environment for people have already been improved over the years. These demands, however, post an escalating threat of global warming and ozone depletion due to harmful emissions of greenhouse gases. In order to reduce these effects, an alternative cooling such as adsorption chiller is required. The main components of the chiller are the evaporator, the condenser and two or more adsorption beds. The adsorption bed is fin-tube based heat exchanger, where the adsorbent materials are housed with stainless steel mesh [1]. The supply of solar radiation or waste heat is required to drive the adsorption chiller, which comprises the operating principles of "adsorption-triggered-evaporation" and "desorption-activated-condensation" [2, 3]. Water is usually preferred to be the adsorbate as it is non-toxic, easily available and has a high latent heat of evaporation. For more water uptake and faster kinetics, the adsorbent materials should be porous structure with higher pore volume and narrower pore width [4]. At present, the commercially available adsorption chillers are designed with silica gels and zeolites [5 – 8], which are hydrophilic in nature at room temperature and also show hydrophobic behaviours at higher temperature.

It should be noted here that a new class of zeolites namely aluminophosphate base AQSOA was developed for desiccant cooling and dehumidification applications [9]. The AQSOA type adsorbents have the ability to desorb water vapour at relatively low temperatures as compared to those of conventional zeolites and silica gels. AQSOA-Z01 is an iron aluminophosphate with the pore width of 7.4Å. AQSOA-Z02 is a silico-aluminophosphate that consists of cages at 3.7Å openings. AQSOA-Z05 is an aluminophosphate having a pore width of 7.4 Å [9]. AQSOA-Z02 is characterised as chabazite (CHA) type molecular sieve with three dimensional structure, and

its surface structural framework consists of AlO_4, PO_4 and SiO_4 tetrahedrons. On the other hand, both AQSOA-Z01 and Z05 are belonged to AFI type molecular sieves that contain tetrahedron openings. It should be noted here that AQSOA-Z01 is a modified version of AQSOA-Z05 with the addition of Fe atoms. Based on experimental data [10-12], it is observed that AQSOA type zeolites such as Z01, Z02 and Z05 show ‘‘s-shape’’ isotherm as an indicator of pore filling mechanism. With this characteristic, a sharp rise in equilibrium adsorbate uptake can be found in a narrow range of relative pressure, and the hydrophobic range is increased at higher temperatures.

Shimooka et al. performed the dehumidification performance on AQSOA-Z05 [10] with a fin-tube heat exchanger, and they found that the water sorption capabilities of AQSOA Z05 at lower relative pressure are lower than those of AQSOA-Z01 and AQSOA-Z02. In another study, Goldsworthy showed the water adsorption isotherms of AQSOA zeolites, silica gel type RD and CECA 3A from 40°C to 160°C [11], and these isotherms were fitted with isotherm model of Mosquera [13] based on statistical complex mechanics analysis. Kayal et al. reported a detailed characterisation of AQSOA-Z01 and AQSOA-Z02 types zeolites [12]. Water adsorption isotherms and isotherm fittings were also performed on AQSOA-Z01 and AQSOA-Z02 zeolites using the isotherm model of Sun and Chakraborty [4]. Up to now, a complete study of water adsorption on AQSOA zeolites ranging from Henry’s region to saturated pressure under static and dynamic conditions is not available in literature. Therefore, the study of adsorption under dynamic conditions is the main theme of this paper.

In this paper, the amount of water vapour uptakes on AQSOA-Z01, Z02 and Z05 zeolites are measured by a gravimetric analyser under static and dynamic conditions for the temperature ranging from 298K to 333K with the pressures up to the saturated region. These experimental

data are fitted with the theoretical isotherm equations of Sun and Chakraborty [4], Dubinin-Astakhov [14] and the modified Langmuir equation [15] within acceptable error ranges. Employing the concept of Langmuir kinetics analogy, the theoretical uptake derivations in time domain are expressed, and the simulation results are compared with experimental data. Finally the isosteric heat of adsorption is calculated with respect to pressure-temperature-uptake co-ordinate system.

2. Experimental

Porous Characteristics

The pore volume, pore size and specific surface area of zeolites were measured by N_2 adsorption/desorption isotherms data at 77K. The zeolite samples were degassed at 160°C for 6 hours before N_2 adsorption measurement. The isotherms data were equipped with BET (Brunuer-Emmet-Teller) equation to calculate the BET surface area. The total pore volume is obtained by N_2 adsorption data under saturation conditions. If there is no macropores, the isotherm curve is nearly horizontal and P/P_s approaches to one or the saturated region. However, with the existence of macropores, the N_2 isotherm shows a sharp increase at $P/P_s = 1$. Hence, the limiting uptake of the isotherm is used to identify the total pore volume of adsorbent. Since N_2 is saturated at $P/P_s = 1$, the total pore volume is equivalent to the volume of liquid N_2 (V_{liq}) adsorbed in the adsorbent, and it is calculated by $V_{liq} = \frac{P_a V_{ads} V_m}{RT}$ where V_{ads} is the volume of N_2 adsorbed in adsorbent pores, V_m is the molar volume of liquid N_2 (3.47 x 10^{-5} m^3/mol), P_a and T are ambient pressure and temperature respectively. Employing the known total pore volume and surface area, the average pore size (r_p) can be estimated by $r_p = \frac{2V_{liq}}{A_s}$, where A_s is the BET

surface area. Table 1 shows the porous properties of the AQSOA zeolites. All results are presented in detail in the Supporting document. For comparison purposes, the pore volume and surface area data as found in literature are also furnished in Table 1. Due to the presence of ionic radii of Fe^{3+} and Si^{4+}, both AQSOA-Z01 and AQSOA-Z02 have better porous properties than AQSOA-Z05.

Water Adsorption

The experimental investigations for water adsorption on zeolites samples are carried out by a thermogravimetric analyser. Figure 1 shows the schematic diagram for understanding the measurement of water vapour uptakes at various temperatures and pressures. The dry mass of zeolite sample is firstly measured by using the calibrated moisture balance at 140 ^{o}C until there is no further change in mass. The zeolites are then placed on the sample cell, which is held by a microbalance, located above the adsorption chamber, known as the balance head. It should be noted here that the isothermal environment surrounding the zeolite adsorbent is maintained by direct radiant heating where the heaters are placed outside the hermetic reaction chamber and homogenized by a waft of cooling air through the non-hermetic gap between the chamber and radiant heater. The dry zeolite mass is again confirmed inside the adsorption chamber by direct radiant heating at 140 ^{o}C with continuous supply of helium to remove all moisture from the sample. After regeneration process, the system is ready for the measurement of adsorption isotherms.

The balance head requires to be set at a temperature at least 15°C above the experimental conditions to eliminate the condensation effects in the adsorption chamber. Dry Nitrogen (99.999% purity) is introduced into the adsorption chamber to control buoyancy effects of the balance. The

vapour is generated in a humidifier. The temperature inside the humidifier is measured by a class A RTD temperature sensor with an accuracy of ± 0.15 ^{o}C. The vapour charging flow rate is controlled automatically. The adsorbent is placed in the quartz sample bowl inside the reaction chamber which has a radiant heater for maintaining a constant temperature. A vacuum pump is used for vacuuming and purging the system before an experiment and maintaining the adsorption chamber pressure in coordination with a vacuum controller.

During the adsorption experiment, both the pressure and temperature of the adsorption chamber are controlled within acceptable error ranges. Hence, the temperature probes and the humidity sensor are used to calculate the temperature and relative pressure (P/P_s). The humidity probe stabilises the value of P/P_s in the adsorption chamber by controlling the flow rate of dry N_2. If P/P_s is higher than that of expected values, the flow rates of dry N_2 are increased and the N_2 flow across the humidifier is stopped. The excess water vapour content is purged out of the chamber so that the P/P_s can be obtained at the desired value, which also introduces the right distribution of dry nitrogen to water vapour. If P/P_s is lower, the dry N_2 flow through the humidifier is increased for the addition of water vapour content within the adsorption chamber. The water uptake is measured on the basis of P/P_s and the set temperature of the adsorption chamber. During the adsorption process, the amount of total mass, M_t, is increased due to the addition of water vapour from the humidifier (Figure 1). Subsequently, the M_t of the adsorbent – adsorbate system is further increased as more water vapour is added to the chamber, making M_t a function of pressure. The mass of adsorbate, m_a, at any pressure P_i can be determined by $m_{a,i} = M_t(P_i) - M_t(P_o)$, where i is a variable to signify each pressure point, and $M_t(P_o)$ defines the total mass of zeolite + water vapour at initial known pressure P_o. The mass of adsorbate allows the gravimetric uptake to be calculated by $q_i = m_{a,i}/M_s$ for each pressure point, where

M_s is the mass of dry solid adsorbent. The adsorption kinetic data is also achieved while measuring the water uptake of the adsorbent as a function of time. Adsorption kinetic determines the amount of time taken for the adsorption to reach equilibrium at given temperature and pressure. Thus, at a specific temperature and pressure, the change in mass of adsorbent due to the increment of water vapour uptake is measured with respect to time. For a given temperature, the P/P_s values are varied to attain the water uptakes to form the isotherm. Before achieving the new isotherm data, the adsorbents are retrieved from the adsorption chamber and placed them in an oven at 150°C for regeneration. Then, with the regenerated adsorbent placed into the adsorption chamber, the adsorption chamber is purged with dry nitrogen at 65°C. The experiment is repeatedly performed to ensure that the repeatability is achieved within the experimental uncertainties.

3. Adsorption Isotherm and Kinetic Modelling

The amount of experimentally measured water vapour uptake data under equilibrium and dynamic conditions are fitted with adsorption isotherms and kinetics models as these models are generally utilized to design and simulate adsorption assisted heat transmission system. Various adsorption isotherm models are used to model adsorbent – adsorbate behaviour in a pressure – temperature – uptake coordinate system. From the experimental data, it is found that the adsorption isotherms data of AQSOA-Z01, Z02 and Z05 indicate S-shaped isotherm. Generally, Langmuir, Tóth and Dubinin-Astakhov equations fail to explain the S-shaped isotherm within acceptable error ranges [16]. Recently, Sun and Chakraborty have developed an adsorption isotherm model for explaining S-type isotherm, which is given by [4]

$$\theta = \frac{K(P/P_s)^m}{1+(K-1)(P/P_s)^m} \tag{1}$$

where K is the isotherm coefficient and is defined by $K = \alpha \exp\{m(Q_{st}^* - h_{fg})/RT\}$, α is the pre-exponential coefficient, m defines the surface-structural heterogeneity factor, Q_{st}^* is the isosteric heat of adsorption at zero surface coverage, h_{fg} indicates the enthalpy of evaporation and R is the gas constant. θ is the surface adsorbate coverage and is given by q/q^o, where q is the amount of water vapour uptake and q^o is the limiting uptake. Hence, $(Q_{st}^* - h_{fg})$ resembles to the adsorption characteristics energy and can also be approximated from experimental data. Employing the concepts of Lennard – Jones and electrostatic potentials, the isosteric heat of adsorption at zero coverage (Q^*_{st}) is calculated as a function of pore width [17] or

$$Q^*_{st} = RT - \frac{\int_0^{H_c} V_{ext}(z)\exp\left[-V_{ext}(z)/RT\right]dz}{\int_0^{H_c} \exp\left[-V_{ext}(z)/RT\right]dz}. \quad (2)$$

Hence H_c indicates the pore width and V_{ext} is the adsorbent wall potential as derived by $V_{ext}(z) = U_{sf}(z) + U_{sf}(H - z)$, where H is the distance between the nuclei of the outer adsorbent atoms on opposite walls. The adsorbent-adsorbate interaction potential (U_{sf}) as a function of pore width direction (z) is defined as $U_{sf} = 2\pi\varepsilon_{sf}\rho_s\sigma_{sf}^2\Delta\left[\frac{2}{5}\left(\frac{\sigma_{sf}}{z}\right)^{10} - \left(\frac{\sigma_{sf}}{z}\right)^4 - \frac{\sigma_{sf}^4}{3\Delta(0.61\Delta + z)^3}\right]$ [18], where σ_{sf} and ε_{sf} are the solid-fluid collision diameter and the solid-fluid well depth potential, respectively. Δ defines the separation between the adsorbent planes and ρ_s is the density of solid adsorbent. For water adsorption cases: σ_{sf} = 3.43 Å, ε_{sf} = 8.119 × 10^{-21} J/mol, Δ = 3.35 Å and ρ_s = 0.055 [4].

The experimentally measured water uptakes data are also fitted with Dubinin-Astakhov (DA) and the modified Langmuir equation to represent the characteristics curve. Mathematically, the DA equation is given by [14]

$$q = q^{o} \exp\left[-\left\{ \frac{RT}{E} \ln\left(\frac{P_s}{P} \right) \right\}^{n} \right] \tag{3}$$

where E defines the characteristics energy, R is the gas constant, P_s defines the saturated pressure and n is the number of adsorptive sites or heterogeneity coefficient. The modified Langmuir adsorption isotherm equation is formulated on the basis of Fermi-Dirac distribution function, and it includes the loading, the adsorbent-adsorbate interaction and the surface structural heterogeneity factors [15]

$$q = q^{o} \beta \left(\frac{P}{\varphi^{*}} \right) \Bigg/ \left[1 + \left(\beta^{t_1} - \alpha \right) \left(\frac{P}{\varphi^{*}} \right)^{t_1} \right]^{\frac{1}{t_1}}, \tag{4}$$

where $\frac{P}{\varphi^{*}} = \left(\frac{P}{P_s} \right) \exp\left\{ \frac{\phi_m}{RT} \left\{ 1 - \left(\frac{P}{P_s} \right)^{n_1} \right\} + z \right\}$. Here ϕ_m is the minimum potential energy, β is the loading factor, t_1 defines the surface heterogeneity, n_1 is the adsorbate-adsorbent interaction factor and z indicates the compressibility factor.

According to Langmurian theorem, the adsorption equilibrium constant K is expressed in terms of adsorption and desorption rate coefficients k_{ads} and k_{des}, respectively i.e. $K = k_{ads}/k_{des}$. Employing equation (1), the surface coverage (θ) under equilibrium conditions becomes [4]

$$k_{des}\theta\left\{1 - (P/P_s)^{m}\right\} = k_{ads}(1-\theta)(P/P_s)^{m} \tag{5}$$

According to Langmuir [19], adsorption is regarded as a reversible process between adsorbents and adsorbate molecules. Therefore, under non-equilibrium condition, the amount of adsorbate surface coverage as a function of time (θ_t) can be expressed as [20]

$$\frac{d\theta_t}{dt} = k_{ads}(1-\theta_t)\left(\frac{P}{P_s}\right)^m - k_{des}\theta_t\left\{1-\left(\frac{P}{P_s}\right)^m\right\}. \quad (6)$$

With the relation between k_{ads} and gas molecular collision frequency, k_{ads} is calculated as $k_{ads} = W\beta A_s$, where W is the number of collisions of molecules with the surface per unit time, A_s is the specific surface area of the adsorbent and β is the sticking coefficient. The number of collisions of molecules with adsorbent surface is determined by $W = MP/\sqrt{2\pi MRT}$, where M is the molecular weight of molecules in gram per mole. The sticking coefficient is given by $\beta = \{\beta_o \exp(-E_a/RT)\}$, where β_o is the pre-exponential or frequency factor and E_a is the activation energy [21]. By rearranging Equation (6),

$$\begin{aligned}\frac{d\theta_t}{dt} &= k_{ads}\left(\frac{P}{P_s}\right)^m - \theta_t\left\{k_{ads}\left(\frac{P}{P_s}\right)^m + k_{des}\left[1-\left(\frac{P}{P_s}\right)^m\right]\right\} \\ &= k_{ads}\left(\frac{P}{P_s}\right)^m - \theta_t k_{des}\left\{1+(K-1)\left(\frac{P}{P_s}\right)^m\right\} \\ &= k_{ads}\left(\frac{P}{P_s}\right)^m - \theta_t\frac{1}{\tau}\end{aligned} \quad (7)$$

where $1/\tau = k_{ads}(P/P_s)^m + k_{des}\left\{1-(P/P_s)^m\right\}$ is the time constant. The analytical solution of equation (7) becomes $\theta_t = C'e^{\frac{-t}{\tau}} + \frac{k_{ads}(P/P_s)^m}{1/\tau} = C'e^{\frac{-t}{\tau}} + \theta$. Employing the initial condition ($\theta = \theta_{ini}$ at t = 0) of adsorption process, the constant C' is found to be $\theta_{ini} - \theta$. Thus, with rearrangement, the analytical solution is written as

$$\frac{\Delta\theta_t}{\Delta\theta} = 1-\exp(-t/\tau), \quad (8)$$

where $\Delta\theta_t = (\theta_t - \theta_{ini})$ and $\Delta\theta = (\theta - \theta_{ini})$. Hence, θ_{ini} indicates the initial adsorption uptake fraction.

4. Results and Discussion

Employing the pore model and LJ potential theory (equation 2), Q_{st}^* is calculated as a function of pore width. The Q_{st}^* against pore widths of AQSOA (types CHA and AFI) zeolites are shown in Figure 2. A rapid change in Q_{st}^* is occurred for pore sizes ranging from 3.5 Å to 6 Å. The local maxima of AQSOA type zeolite is observed with the minimum pore width of ≈ 4 Å. At that point, the Q_{st}^* is calculated as 4500 kJ/kg for CHA type zeolites namely AQSOA-Z02. The Q_{st}^* is calculated to be 3200 kJ/kg at the pore width of ≈ 4 Å for AFI type zeolites namely AQSOA-Z01 and AQSOA-Z05. The average pore sizes of AQSOA zeolites are found ≈ 11 Å. The LJ parameters are furnished in Table 2 [22 – 25].

Adsorption Isotherms

Figures 3 (a – c) show the experimentally measured data for the adsorption of water vapour on AQSOA-Z01, Z02 and Z05 zeolites under static conditions. The experimental data of Shimooka et al. [10] at 298 K are included here for comparison purposes. From Figure 3(a), the hydrophobic length of AQSOA-Z01 begins from Henry's region to the relative pressure (P/P_s) of 0.1. When P/P_s is higher than 0.1, the water uptake increases sharply. This may be due to the fact that AQSOA-Z01 is mainly fabricated by AlO_4, PO_4 and FeO_4 tetrahedron, and Al and P atoms are partially replaced by Fe atoms. The Fe atoms attract more water molecules at higher pressure due to higher enthalpies of adsorption. On the other hand, Figure 3(b) shows that AQSOA Z02 type zeolite shows a very short hydrophobic length with water adsorption due to the presence of

SiO_4 tetrahedrons. With the presence of SiO_4 in AQSOA-Z02 zeolite structure, water molecules are attracted towards this adsorbent at lower relative pressure as Si atoms has higher affinity with water. Similarly at the higher temperature of 333K, the isotherm also shows a short hydrophobic length at lower relative pressure. By considering the short hydrophobic length at lower pressure AQSOA-Z02 + water system provides S-shape or type V isotherm and indicates the presence of a pore filling phenomena. The isotherms at very low pressures are also shown in Figure 3(b). Figure 3(c) indicates that AQSOA-Z05 has longer hydrophobic length up to the relative pressure of 0.2 due to the absence of both Fe and Si atoms in AQSOA-Z05 structures. The crystal structure of Z05 consists mainly of AlO_4 and PO_4 tetrahedrons only. Hence, the experimental data are fitted with the isotherm model of equation (1) to calculated isotherm parameters for AQSOA zeolites + water systems. Figure 3(a) indicates that the isotherm model is closely fitted with the experimental data within 5% error margins both in the Henry and saturated pressure regions. However, the errors are higher than 8% for the relative pressure ranging from 0.1 to 0.3. It is also found from Figure 3(b) that equation (1) shows a better curve-fitting (error within 5%) for AQSOA-Z02 + water system as compared with other isotherms. Figure 3(c) indicates the S-shaped isotherm phenomenon, where the isotherm model of equation (1) provides relatively higher errors (errors > 5%) for the relative pressures varying from 0.1 to 0.3. For water adsorption, the isosteric heat at zero coverage $\left(Q_{st}^{*}\right)$ is calculated by equation (2). It should be noted here that α is related to the entropy of adsorption and the m is responsible for the shape of the isotherm curve. From isotherm data, it is found that the hydrophobic length of AQSOA Z01 and Z05 depends on m significantly. Table 3 shows the parameters of equation (1) for AQSOA type zeolites + water systems. Hence the experimentally measured isotherm data are also fitted with Dubinin-Astakhov (DA) and the modified Langmuir equations. Both DA and Langmuir

equations are able to handle the experimental data between 298 K and 318 K within experimental uncertainties as these equations are formulated from the rigor of micro-pore filling theory. However, DA and modified Langmuir equations are not worked well at higher temperature adsorption. The parameters of DA and the modified Langmuir isotherm equations are also listed in Table 3.

For understanding the hysteresis behaviours, the experimentally measured adsorption – desorption isotherms for AQSOA type zeolites (Z01, Z02 and Z05) and water systems at 298 K are plotted in Figure 4. Hence, for each AQSOA-zeolite + water system, the uptakes are measured in the direction of adsorption as the amount of water vapor uptake is increased with pressure. When the equilibrium is achieved at the maximum uptake point, the system is depressurized and the uptakes ate measured and recorded in the direction of desorption. In the present experiment the adsorption–desorption cycle is repeated at least two times to establish the repeatability experimental data. The first adsorption curve is obtained by the adsorption of water vapour on anhydrous zeolite, and the second curve is obtained from the fully hydrated zeolites. A hysteresis behavior in the adsorption-desorption curve is observed at very low pressures. This occurs due to the fact that the desorption process is not completed. Some residual water remains trapped in the porous AQSOA zeolites even when the pressure is low. For all adsorption-desorption diagrams, the hysteresis effect is not large at higher relative pressures, which indicates a narrow distribution of relatively uniform pores.

Adsorption Kinetics

The amount of water vapour uptakes on AQSOA-type Z01, Z02 and Z05 zeolites for the temperatures of 298 K and 333 K under dynamic conditions are shown in Figures 5(a), 5(b) and

5(c). The adsorption kinetics model as presented in equation (8) is fitted with experimental data within acceptable error ranges (± 5%). The kinetic parameters are furnished in Table 4. The adsorption equilibrium coefficient, K, is used to calculate k_{ads} and k_{des} of the kinetic model. Hence, the exponential coefficient β_o is considered 1 due to monolayer adsorption capacity according to experimental setup. It should be noted that the value of β_o depends on the size and layer of solid adsorbents [20]. The activation energy of the AQSOA zeolites with water (E_a) ranges from 32000 to 54000 J/mol. Figures 5 (a – c) show that AQSOA Z01 has relatively longer time to reach equilibrium as compared to Z02 and Z05. The presence of more Si atoms in AQSOA Z02 structure ensures a high interaction between the adsorbent and water at low relative pressure. These results also suggest that a longer cycle time for AQSOA Z01+ water system can be implemented if AQSOA-Z01 is used as adsorbent for the design of adsorption chiller. It should be noted here that the linear driving force (LDF) model over-estimates the adsorption rate as it does not consider the pressure effects [26]. It is observed that k_{ads}, k_{des} and τ depend on temperature and pressure. However the value of activation energy E_a, m and K are constant. This means that isotherm parameters are used to calculate the time constant, τ i.e, water vapour uptakes and off-takes as a function of time. Hence the value of β_o is considered 1 due to experimental condition (thin AQSOA zeolite layer is deemed). For more layers of zeolites especially in practical applications the value of $\beta_o < 1$ [20].

Isosteric Heat of Adsorption

As very large hysteresis is not observed for the adsorption and desorption of AQSOA zeolites and water system. Therefore, the Clausius Clapeyron equation can be applied to predict the isosteric heat, Q_{st}. The experimental data of zeolites + water system related to the increase in

temperature with pressure are logged for various amounts of water uptakes. A plot of ln(P) versus (1/T) for the adsorption of water on AQSOA-Z01 is shown in Figure 6. All experimental data produce straight lines with higher regression coefficients. The slopes of these straight lines determine the values of $-Q_{st}/R$, where R is the gas constant. A detailed analysis is presented in the supporting document. The Q_{st} results for AQSOA-Z01, Z02 and Z05 with water are shown in Figure 7. A sharp rise in Q_{st} is found from Henry's region to the uptake of 0.05 kg/kg for the adsorption of water on AQSOA-Z02 zeolite. The increment of Q_{st} becomes smoother as the uptake is further increased. The reason is that the water molecules adsorb rapidly onto sites of higher energy, and as adsorption progress, water is adsorbed onto the lower energy sites. At first, the water molecule enters into narrower pores and due to the presence of Si atoms, strong interactions between water molecules and AQSOA-Z02 are occurred. Therefore, the Q_{st} increases sharply at smaller uptake. Once the smaller pores are filled, water molecules start to occupy the larger pore of the adsorbents. Unlike AQSOA-Z02, AQSOA-Z01 and AQSOA-Z05 have slightly higher Q_{st} at the Henry's region. As adsorption progress, Q_{st} increases sharply up to the uptake of 0.15 kg/kg for AQSOA-Z01 and 0.18 kg/kg for AQSOA-Z05 zeolites. Due to the hydrophobic nature of AQSOA-Z01 and Z05 adsorbents, water is adsorbed at higher energy sites of AQSOA materials at first. It should be noted here that the same Q_{st} trends are observed for both AQSOA-Z01 and Z05 adsorbents. However the Q_{st} values of AQSOA-Z01 + water system are higher than those of AQSOA-Z05 + water system. This is due to the fact that AQSOA-Z01 consists of Fe atoms and Fe absorbs more water molecules with relatively higher energies.

5. Conclusions

The isotherms and kinetics data for three different AQSOA type zeolites (Z01, Z02 and Z05) are experimentally measured by a gravimetric method. This study provides detailed experimental and theoretical findings of the AQSOA zeolites for water adsorption process. The experimental results ranging from the Henry's region to the saturated pressure are fitted with various isotherm and kinetics models within acceptable uncertainties of ± 5%. However, the uncertainties are varied from ± 2 to ± 10%. The kinetic model is derived from Langmurian analogy and the adsorption and desorption rates are calculated from the concept of adsorption isotherm coefficient (*K*), which provides better approximations as compared with the conventional liner driving force (LDF) model. The isosteric heat at zero coverage is also calculated from LJ and electrostatic potentials model. The adsorption isotherms are applied for the modelling of adsorption processes such as those occurring in, for example, adsorption chillers or desiccant wheels or adsorption desalination. The isosteric heat in a pressure-temperature-uptake co-ordinate system is needed for the prediction of system performances. The kinetics data of zeolites + water systems show a realistic situation of compact adsorption heat exchanger (finned tube type) in which single or multi-layer zeolites is housed. The kinetic study is essential for designing the dynamic behaviours of adsorption device with respect to the optimum adsorption-desorption time under transient or batch operating conditions. This study provides an explanation for calculating the rate of water vapour uptakes on various AQSOA-type zeolites in terms of pressure and temperature.

Nomenclature

A_s	BET surface area,	m^2/kg
E_a	activation energy,	J/mol

h_{fg}	latent heat of vaporisation	kJ/kg
K	Langmuir coefficient	
k_{ads}	adsorption rate coefficient	g/g s^{-1}
k_{des}	desorption rate coefficient	g/g s^{-1}
m	heterogeneity parameter	
P	pressure	kPa
P_s	saturated pressure	kPa
P_a	ambient pressure	
q	amount of water vapour uptake	
q_o	limiting uptake	
Q_{st}	isosteric heat of adsorption	kJ/kg
Q_{st}^*	isosteric heat of adsorption in Henry's region	kJ/kg
r_p	average pore size	Å
R	gas constant	
T	temperature	K
t	time	s
v_p	pore volume	cm^3/g
V_{liq}	volume of liquid N_2	m^3
V_{ads}	volume of N_2 adsorbed	m^3
V_m	molar volume of liquid N_2, 3.47 x 10^{-5}	m^3/mol

Symbol

α	pre-exponential coefficient (isotherm model)

ACCEPTED MANUSCRIPT

β	sticking coefficient
β_o	pre-exponential coefficient (sticking coefficient)
τ	time constant, s
θ	adsorption uptake fraction
θ_{ini}	initial adsorption uptake fraction
θ_t	real time adsorption uptake fraction

Acknowledgments

The authors acknowledge the financing support from Ministry of Education (MOE), Singapore (grant no. MOE 2014-T2-2-061).

References

1. Q. W. Pan, R. Z. Wang, L. W. Wang, and D. Liu, Design and experimental study of a silica gel-water adsorption chiller with modular adsorbers, International Journal of Refrigeration, vol. 67, pp. 336-344, 2016.
2. B. B. Saha, A. Akisawa, and T. Kashiwagi, Silica gel water advanced adsorption refrigeration cycle, Energy, vol. 22, pp. 437-447, 1997.
3. Ang Li, Azhar Bin Ismail, Kyaw Thu, Kim Choon Ng' , Wai Soong Loh, Performance evaluation of a zeolite–water adsorption chiller with entropy analysis of thermodynamic insight, Applied Energy, Vol. 130, pp. 702–711, 2014.
4. B. Sun and A. Chakraborty, Thermodynamic formalism of water uptakes on solid porous adsorbents for adsorption cooling applications, Applied Physics Letters, vol. 104, p. 201901, 2014.

5. S. Graf, F. Lanzerath, A. Sapienza, A. Frazzica, A. Freni, and A. Bardow, Prediction of SCP and COP for adsorption heat pumps and chillers by combining the large-temperature-jump method and dynamic modeling, Applied Thermal Engineering, vol. 98, pp. 900-909, 2016.
6. L. W. Wang, R. Z. Wang, and R. G. Oliveira, A review on adsorption working pairs for refrigeration, Renewable and Sustainable Energy Reviews, vol. 13, pp. 518-534, 2009.
7. A. Freni, L. Bonaccorsi, E. Proverbio, G. Maggio, G.Restuccia, Zeolite synthesised on copper foam for adsorption chillers: A mathematical model, Microporous and Mesoporous Materials, Vol. 120, pp. 402-409, 2009.
8. K. Thu, B. B. Saha, K. J. Chua, K. C. Ng, Performance investigation of a waste heat-driven 3-bed 2-evaporator adsorption cycle for cooling and desalination, International Journal of Heat and Mass Transfer, Vol. 101, pp. 1111 - 1122, 2016.
9. K. Okamoto, M. Teduka, T. Nakano, S. Kubokawa, H. Kakiuchi, The development of AQSOA water vapor adsorbent and AQSOA coated heat exchanger, Innovative Materials for Processes in Energy Systems for Fuel Cells, heat pumps and Sorption Systems, pp. 27 - 31, 2010.
10. S. Shimooka, K. Oshima, H. Hidaka, T. Takewaki, H. Kakiuchi, A. Kodama, M. Kubota, H. Matsuda, The Evaluation of Direct Cooling and Heating Desiccant Device Coated with FAM, Journal of Chemical Engineering of Japan, vol. 40, pp. 1330-1334, 2007.
11. M. J. Goldsworthy, Measurements of water vapour sorption isotherms for RD silica gel, AQSOA-Z01, AQSOA-Z02, AQSOA-Z05 and CECA zeolite 3A, Microporous and Mesoporous Materials, vol. 196, pp. 59-67, 2014.

12. S. Kayal, S. Baichuan, and B. B. Saha, Adsorption characteristics of AQSOA zeolites and water for adsorption chillers, International Journal of Heat and Mass Transfer, vol. 92, pp. 1120-1127, 2016.
13. M. A. Mosquera, Simple isotherm equations to fit type I adsorption data, Fluid Phase Equilibria, vol. 337, pp. 174-182, 2013.
14. D. D. Duong, Adsorption analysis: Equilibria and Kinetics: London : Imperial College Press, c1998., 1998.
15. A. Chakraborty and B. Sun, An adsorption isotherm equation for multi-types adsorption with thermodynamic correctness, Applied Thermal Engineering, vol. 72, pp. 190-199, 2014.
16. M. Khalfaoui, S. Knani, M. Hachicha, and A. Lamine, New theoretical expressions for the five adsorption type isotherms classified by BET based on statistical physics treatment, Journal of Colloid and Interface Science, vol. 263, pp. 350–356, 2003.
17. W. Fan, A. Chakraborty, Investigation of the Interaction of Polar Molecules on Graphite Surface: Prediction of Isosteric Heat of Adsorption at Zero Surface Coverage, Journal of Physical Chemistry C, Vol. *120*, pp 23490–23499, 2016.
18. J. Liu, M. D. LeVan, Henry's Law Constants and Isosteric Heats of Adsorption at Zero Loading for Multi-Wall Carbon Surfaces with Different Geometries, Carbon. Vol. *48*, pp. 3454-3462, 2010.
19. Y. Liu, L. Shen, From Langmuir kinetics to first- and second-order rate equations for adsorption. Langmuir, Vol. 24, pp. 11625–30, 2008.
20. B. Sun and A. Chakraborty, Thermodynamic frameworks of adsorption kinetics modeling: Dynamic water uptakes on silica gel for adsorption cooling applications, Energy, vol. 84, pp. 296-302, 2015.

21. L. D. Asnin, Y. S. Chekryshkin, A. A. Fedorov, Calculation of the sticking coefficient in the case of the linear adsorption isotherm. Russ Chem Bull, Vol.52:2747–2749, 2003.
22. A. K. Rappe, C. J. Casewit, K. S. Colwell, W. A. GoddardIII, W. M. Skiff, UFF, a Full Periodic Table Force Field for Molecular Mechanics and Molecular Dynamics Simulations, Journal American Chemistry Society, Vol. 114, pp.10024 - 10035, 1992.
23. Tatiana M. C. Faro, Gilmar P. Thim, Munir S. Skaf, A Lennard-Jones plus Coulomb potential for Al 3 + ions in aqueous solutions. The Journal of Chemical Physics, Vol. 132, pp. 114509, 2010.
24. Jin-Wu Jiang and Harold S. Park. A Gaussian treatment for the friction issue of Lennard-Jones potential in layered materials: Application to friction between graphene, MoS2, and black phosphorus. Journal of Applied Physics, Vol. 117, pp. 124304, 2015.
25. P. G. Kusalik and I. M. Svishchev, The spatial structure in liquid water, Science, Vol. 265, pp. 1219-1221, 1994.
26. K. Chihara, M. Suzuki, Air Drying By Pressure Swing Adsorption, Journal of Chemical Engineering of Japan, Vol. 16, pp. 293-299, 1983.

ACCEPTED MANUSCRIPT

List of Tables

Table 1: Porous Properties of AQSOA type Z01, Z02 and Z05 zeolites

Type	Pore Volume (cm^3/g)	BET Surface Area (m^2/g)	Average Pore Size (Å)
AQSOA-Z01	0.071 0.087 [12]	189.6 132 [12] *130 – 250	11.78
AQSOA-Z02	0.27 0.2769 [12]	717.8 590 [12] *650 – 770	11.84
AQSOA-Z05	0.07	187.1 *210 – 330	11.76

*Manufacturer data

ACCEPTED MANUSCRIPT

Table 2: LJ parameters for the calculation of isosteric heat at zero coverage

AFI type zeolites (AQSOA-Z01 and 05): mainly $AlPO_4$ and water			
Atom i	Atom j	σ(Å)	ε (K)
Al-$AlPO_4$	Al-$AlPO_4$	4.008	82.95
P-$AlPO_4$	P-$AlPO_4$	3.694	184.97
O-$AlPO_4$	O-$AlPO_4$	3.118	22.98
O-H_2O	O-H_2O	3.16	78.21
Al-$AlPO_4$	O-H_2O	3.584	80.54
P-$AlPO_4$	O-H_2O	3.427	120.28
O-$AlPO_4$	O-H_2O	3.139	42.39
CHA type zeolites (AQSOA-Z02): mainly SiO_2 and water			
Atom i	Atom j	σ(Å)	ε (K)
Si-SiO_2	Si-SiO_2	3.826	202.29
O-SiO_2	O-SiO_2	3.118	30.193
O-H_2O	O-H_2O	3.16	78.212
Si-SiO_2	O-H_2O	3.493	125.785
O-SiO_2	O-H_2O	3.139	48.595

ACCEPTED MANUSCRIPT

Table 3: Parameters of isotherm equations for various AQSOA zeolites – water systems

Isotherm equation (1)				
System	q^o (kg /kg)	Q^*_{st} (kJ/kg)	m	α
AQSOA-Z01 + Water	0.215	3030	4.9	9.0×10^{-7}
AQSOA-Z02 + Water	0.29	4560	1.01	7.0×10^{-6}
AQSOA-Z05 + Water	0.22	2800	6.55	6.77×10^{-5}

Dubinin Astakhov (DA) equation			
System	q^o (kg /kg)	E (J/mol)	n
AQSOA-Z01 + Water	0.21	4000	5
AQSOA-Z02 + Water	0.285	7600	2.9
AQSOA-Z05 + Water	0.22	2700	6

Modified Langmuir isotherm equation							
System	q^o (kg/kg)	z	β	α	t_1	n_1	ϕ_m (J/mol)
AQSOA-Z01 + Water	0.21	3	0.6	0.002479	2	-1.5	520
AQSOA-Z02 + Water	0.29	2.6	0.5	0.005517	2	0.5	250
AQSOA-Z05 + Water	0.22	3	1	0.011109	1.5	-3.5	250

ACCEPTED MANUSCRIPT

Table 4: Parameters of adsorption kinetics for various AQSOA type zeolites – water systems

System	k_{ads} (1/s)	β_o	E_a (J/mol)
AQSOA-Z01 + Water	$3526.81\left(\frac{\beta_o.P}{\sqrt{T}}\right)\exp\left(\frac{-E_a}{RT}\right)$	1	33480
AQSOA-Z02 + Water	$12993.5\left(\frac{\beta_o.P}{\sqrt{T}}\right)\exp\left(\frac{-E_a}{RT}\right)$	1	52250
AQSOA-Z05 + Water	$3471.12\left(\frac{\beta_o.P}{\sqrt{T}}\right)\exp\left(\frac{-E_a}{RT}\right)$	1	38700
$K = k_{ads}/k_{des}$. Hence the pressure P is in Pa and the temperature T is in K. The isotherm coefficient K is obtained from equation 1.			

ACCEPTED MANUSCRIPT

List of Figures

Figure 1: Schematic diagram of gravimetric analyser for the measurement of water uptakes on AQSOA type zeolites under static and dynamic conditions.

Figure 2: Isosteric heat at zero coverage as a function a pore width for AFI (AQSOA-Z01 and Z05) and CHA (AQSOA-Z02) type zeolites.

Figure 3: Experimentally measured water uptakes on (a) AQSOA-Z01, (b) AQSOA-Z02 and (c) AQSOA-Z05 zeolites under static conditions. These data are fitted with various adsorption isotherm models. (●) indicates manufacturer data at 298 K [9] (Figure 3a). (●) also indicates the experimental data of Shimooka et al. at 298 K [10] (Figure 3 c).

Figure 4: Adsorption-desorption behaviour of AQSOA (Z01, Z02 and Z05) zeolites and water systems for the pressures ranging from Henry's region to the saturated pressure at the temperature of 298 K.

Figure 5: Adsorption kinetics of AQSOA zeolites – water working pair. Hence both the experimental data and kinetics simulation results are shown.

Figure 6: A plot of ln(P) versus (1/T) as a function of uptake is shown for AQSOA-Z01 and water system.

Figure 7: Isosteric Heat of Adsorption for AQSOA type (Z01, Z02 and Z05) zeolites – water working pairs.

ACCEPTED MANUSCRIPT

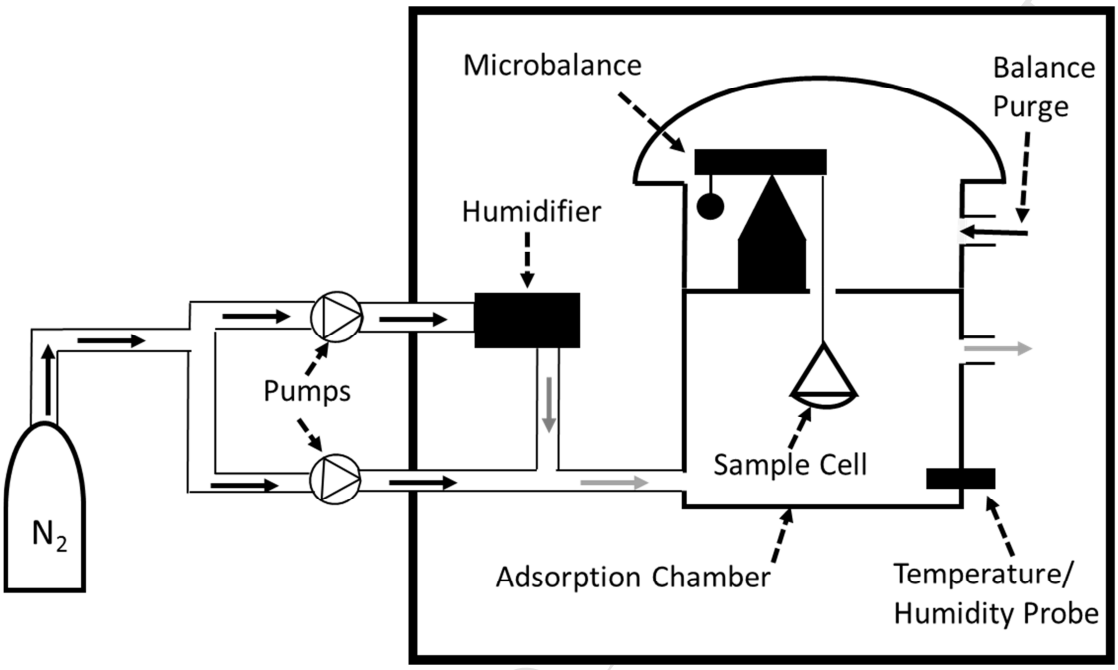

Figure 1

ACCEPTED MANUSCRIPT

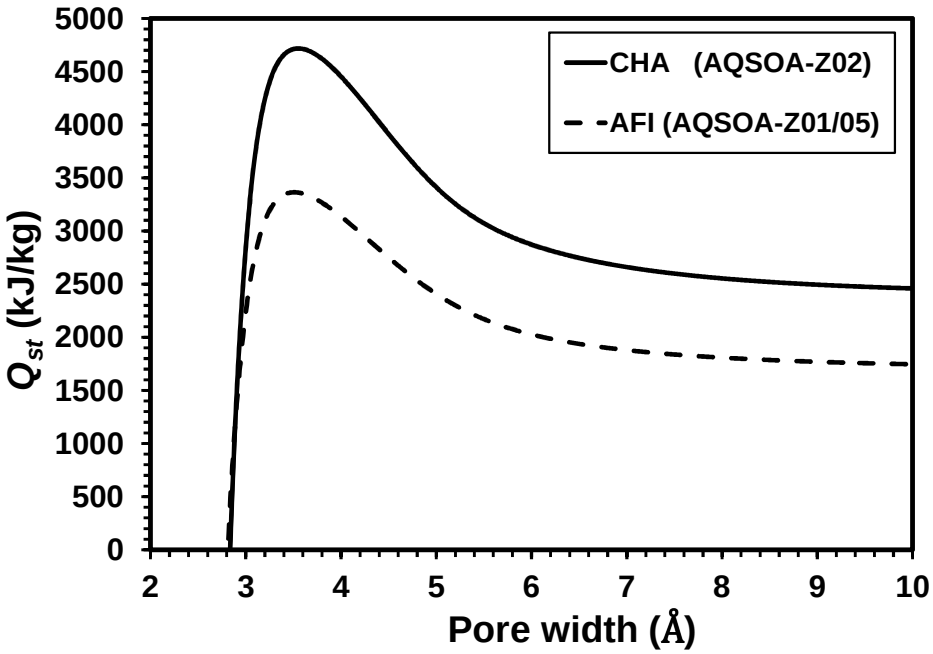

Figure 2

ACCEPTED MANUSCRIPT

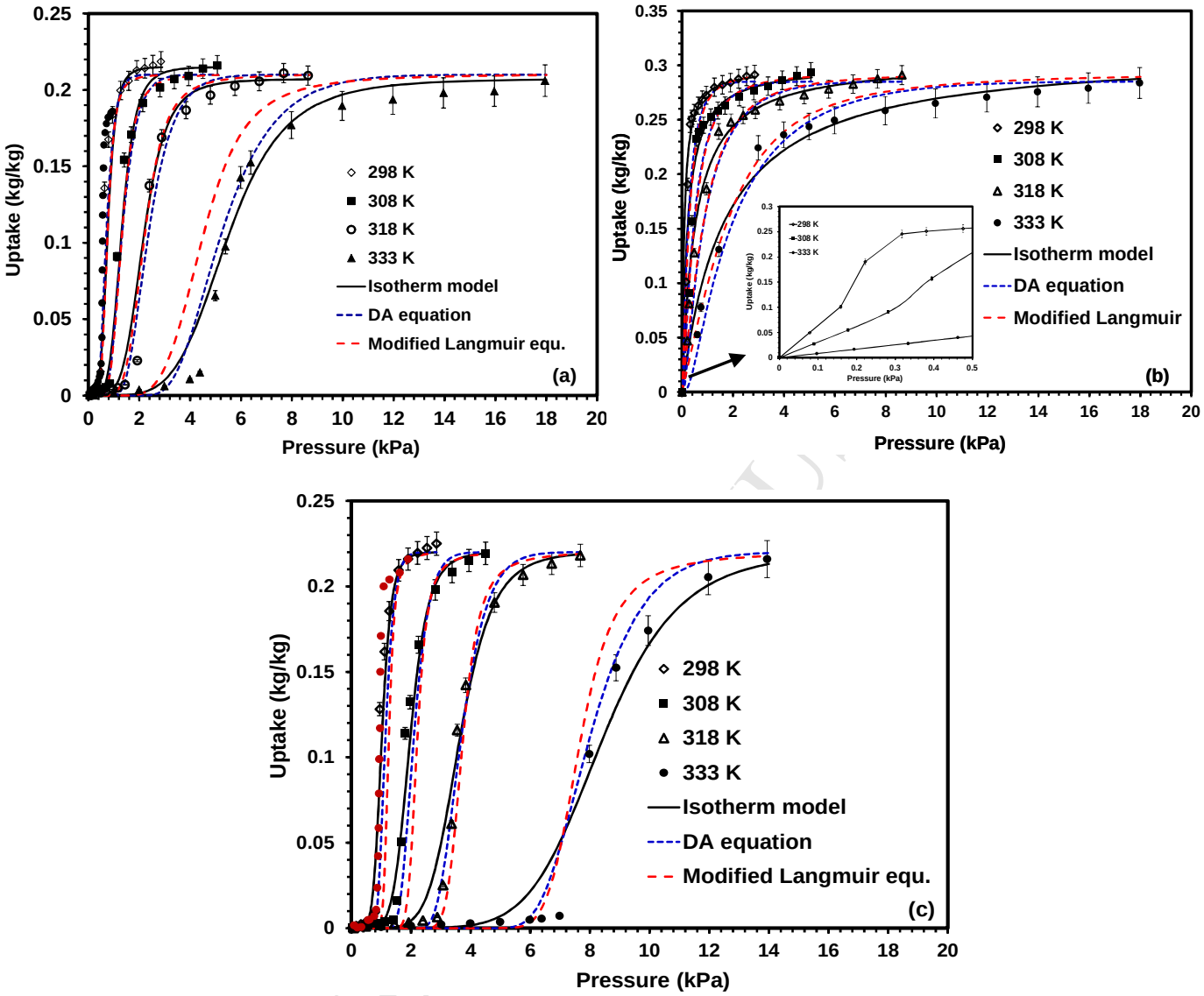
Uptake (kg/kg)
Pressure (kPa)
298 K
308 K
318 K
333 K
Isotherm model
DA equation
Modified Langmuir equ.
(a)
Modified Langmuir
(b)
(c)

Figure 3

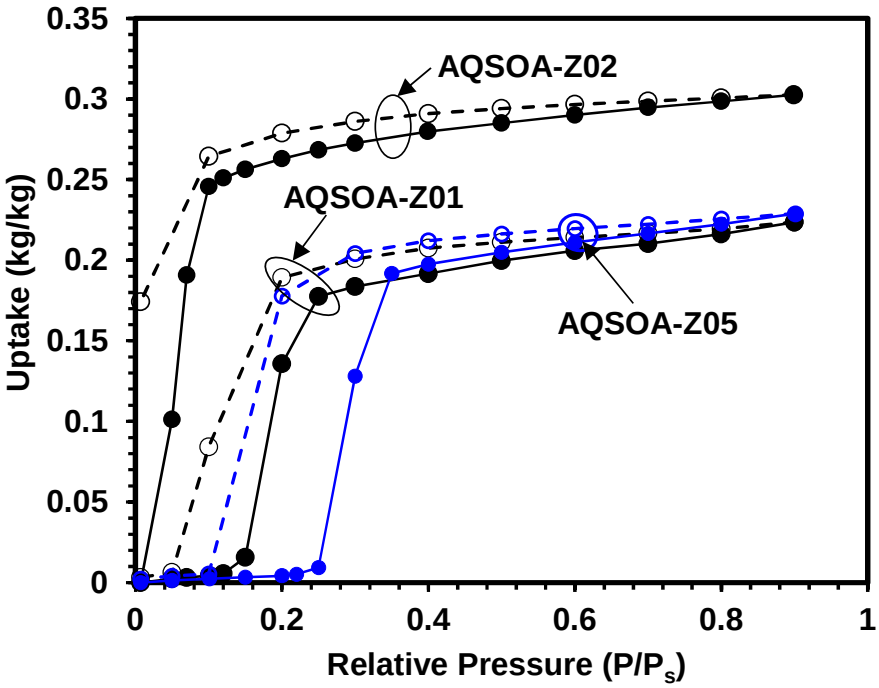
AQSOA-Z02
AQSOA-Z01
AQSOA-Z05
Uptake (kg/kg)
Relative Pressure (P/P$_s$)
0.35
0.3
0.25
0.2
0.15
0.1
0.05
0
0
0.2
0.4
0.6
0.8
1

Figure 4

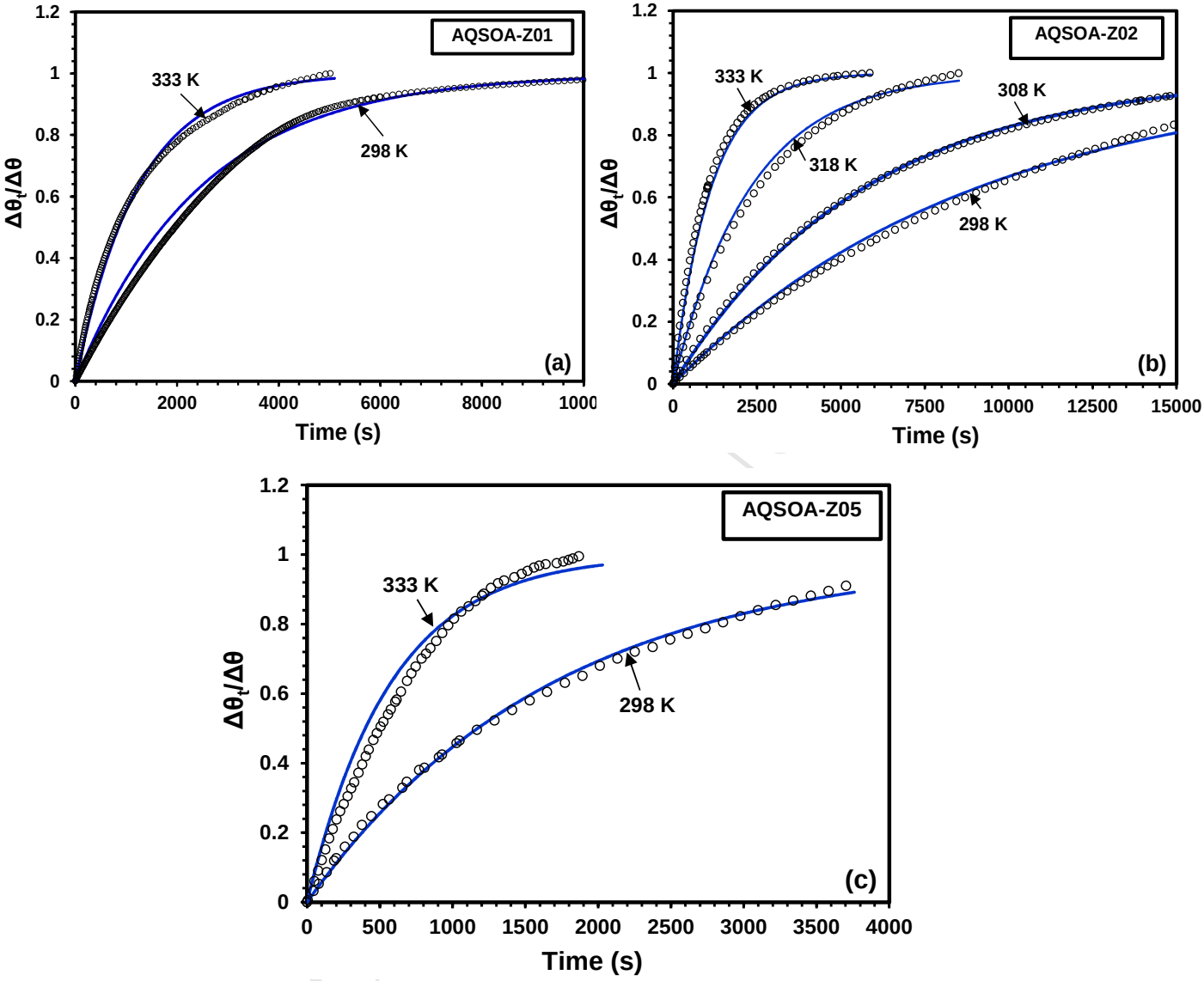
AQSOA-Z01
333 K
298 K
(a)
$\Delta\theta_t/\Delta\theta$
Time (s)
AQSOA-Z02
333 K
318 K
308 K
298 K
(b)
$\Delta\theta_t/\Delta\theta$
Time (s)
AQSOA-Z05
333 K
298 K
(c)
$\Delta\theta_t/\Delta\theta$
Time (s)

Figure 5

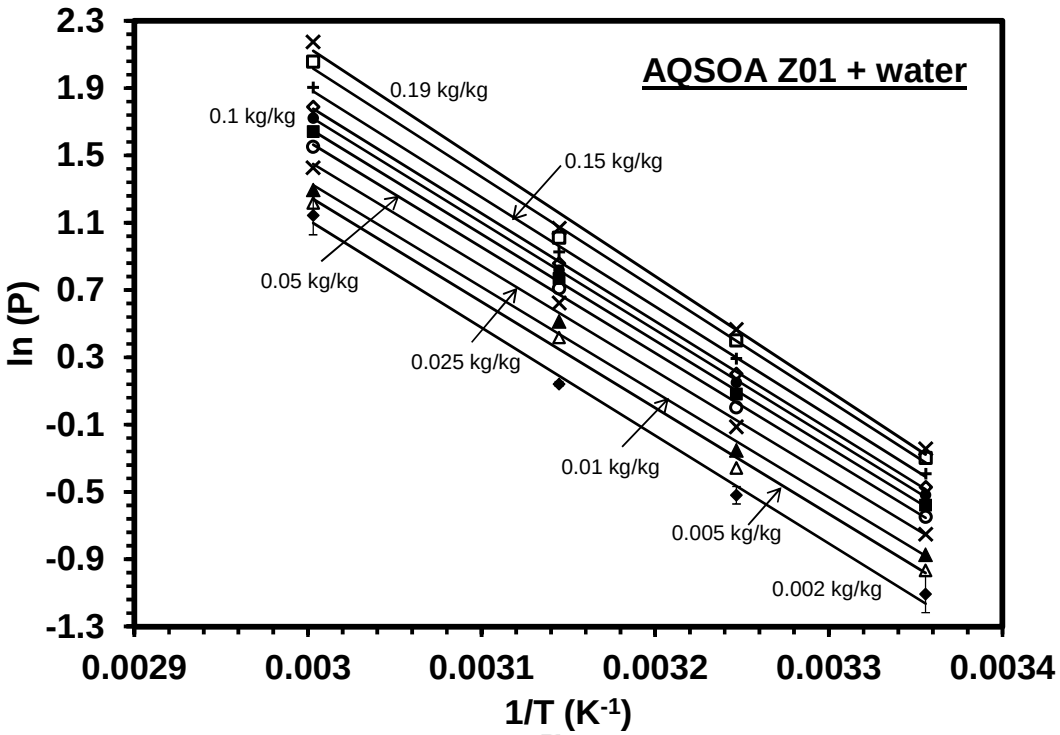

Figure 6

ACCEPTED MANUSCRIPT

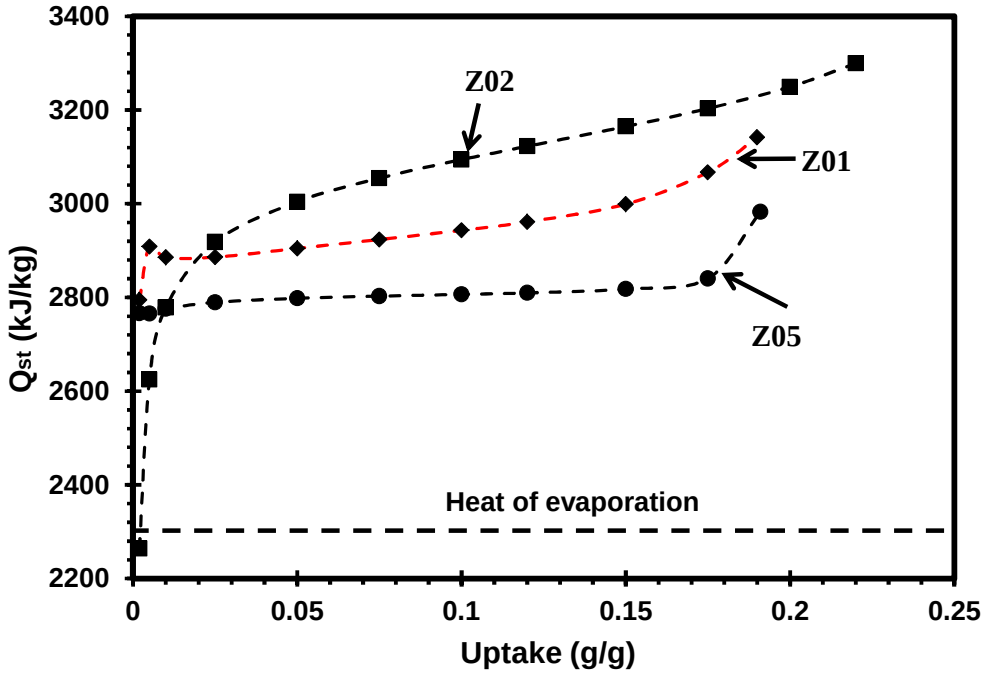
3400
3200
3000
2800
2600
2400
2200
Qst (kJ/kg)
0
0.05
0.1
0.15
0.2
0.25
Uptake (g/g)
Z02
Z01
Z05
Heat of evaporation

Figure 7

ACCEPTED MANUSCRIPT

Improved Adsorption Characteristics Data for AQSOA Types Zeolites and Water Systems under Static and Dynamic Conditions

How Wei Benjamin Teo[1], Anutosh Chakraborty[1,*], Wu Fan[1]

[1]School of Mechanical and Aerospace Engineering, Nanyang Technological University, 50 Nanyang Avenue Singapore, 639798

[*]Author to whom correspondence should be addressed,

E-mail: AChakraborty@ntu.edu.sg, Tel: +65 6790 4222

Highlights

- Water adsorption on AQSOA type zeolites is presented.
- Dynamic behaviours of AQSOA-zeolites + water are presented.
- The kinetics is explained employing Langmurian analogy instead of LDF model.
- The isotherm coefficient K is expressed by adsorption and desorption rates or $K = k_{ads}/k_{des}$.
- Isosteric heat of adsorption for AQSOA zeolites + water is presented as a function of pore widths.

ACCEPTED MANUSCRIPT